Electronic Supplementary Material (ESI) for Journal of Materials Chemistry B.
This journal is © The Royal Society of Chemistry 2015

L-Glutamic Acid Release from a series of Aluminium-based Isoreticular Porous Coordination Polymers

Masashi Nakahama, [a] Julien Reboul, [b] Kenji Yoshida, [a] Shuhei Furukawa, [*,b] and Susumu Kitagawa, [*,a,b]

[a]Department of Synthetic Chemistry and Biological Chemistry, Graduate School of Engineering, Kyoto University, Katsura, Nishikyo-ku, Kyoto 615-8510, Japan

[b]Institute for Integrated Cell-Material Sciences (WPI-iCeMS), Kyoto University, Yoshida, Sakyo-ku, Kyoto 606-8501, Japan

Contents

Fraction of ionic species of guest molecules

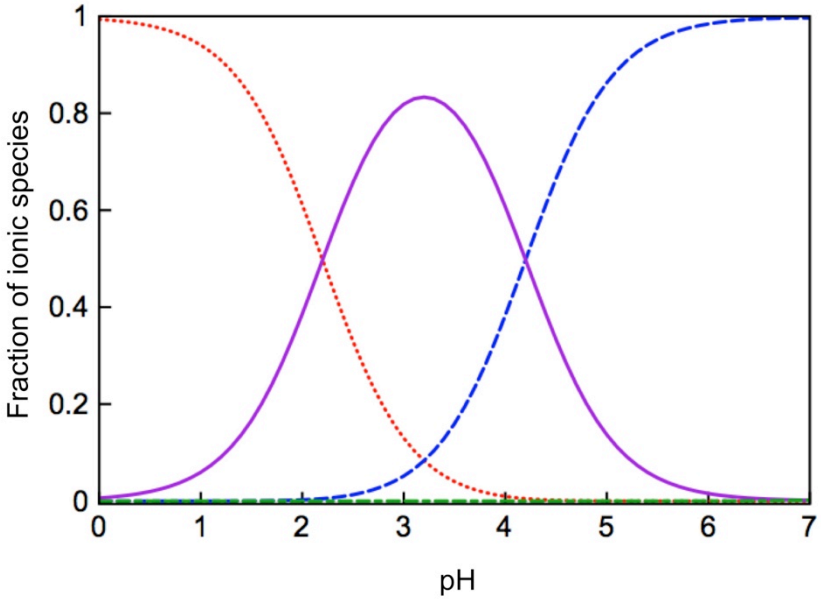

Fig. S1. Fraction of ionic species of Glu under various pH conditions: $GluH_3^+$ (Red), $GluH_2$ (Purple), $GluH^-$ (Blue) and Glu^{2-}(Green).

The calculation of fraction of each ionic species.

Each ionic form of Glu in solution is defined as follows:

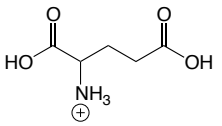

: $GluH_3^+$

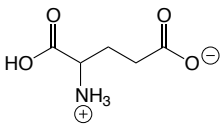

: $GluH_2$

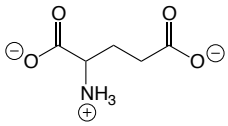

: $GluH^-$

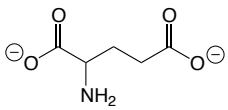

: Glu^{2-}

The acid dissociation of Glu is described as follows:

$$GluH_3^+ \underset{K_1}{\rightleftharpoons} H^+ + GluH_2$$

$$GluH_2 \underset{K_2}{\rightleftharpoons} H^+ + GluH^-$$

$$GluH^- \underset{K_3}{\rightleftharpoons} H^+ + Glu^{2-}$$

Equilibrium constants (K1, K2 and K3) are given by equation (1), (2) and (3), respectively:

$$K_1 = \frac{[H^+][GluH_2]}{[GluH_3^+]} \quad (1)$$

$$K_2 = \frac{[H^+][GluH^-]}{[GluH_2]} \quad (2)$$

$$K_3 = \frac{[H^+][Glu^{2-}]}{[GluH^-]} \quad (3)$$

The mass balance of Glu is described as follows:

$$[GluH_3^+]+[GluH_2]+[GluH^-]=1 \quad (4)$$

Fraction of each ionic forms are allowed by combination of equation (1), (2), (3) and (4).

$$[GluH_3^+] = \frac{[H^+]^3}{A}$$

$$[GluH_2] = \frac{K_1K_2[H^+]}{A}$$

$$[GluH^-] = \frac{K_1[H^+]^2}{A}$$

$$[Glu^{2-}] = \frac{K_1K_2K_3}{A}$$

where A is given by following equation:

$$A=[H^+]^3+K_1[H^+]^2+K_1K_2[H^+]+K_1K_2K_3$$

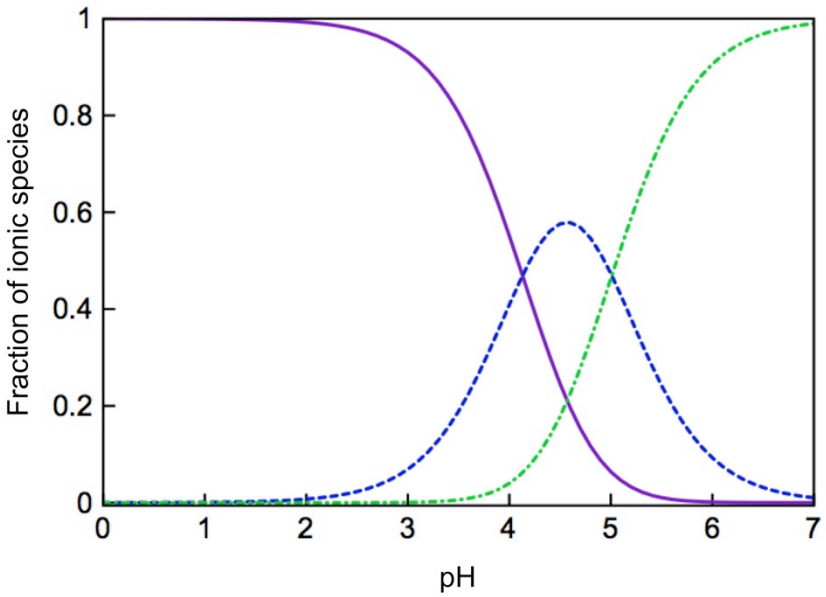

Fig. S2. Fraction of ionic species of Glt under various pH conditions: $GluH_2$ (Purple), $GluH^-$ (Blue) and Glu^{2-} (Green).

The calculation of fraction of each ionic species.

Each ionic form of Glt in solution is defined as follows:

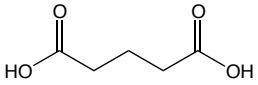 : $GltH_2$

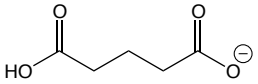 : $GltH^-$

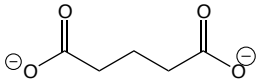 : Glt^{2-}

The acid dissociation of Glt is described as follows:

$$GltH_2 \underset{K_1}{\rightleftharpoons} H^+ + GltH^-$$

$$GltH^- \underset{K_2}{\rightleftharpoons} H^+ + Glt^{2-}$$

Equilibrium constants (K1 and K2) are given by equation (1) and (2), respectively:

$$K_1 = \frac{[H^+][GltH^-]}{[GltH_2]} \quad (1)$$

$$K_2 = \frac{[H^+][Glt^{2-}]}{[GltH^-]} \quad (2)$$

The mass balance of Glt is described as follows:

$$[Glt^{2-}]+[GltH^-]+[Glt^{2-}]=1 \quad (3)$$

Fraction of each ionic forms are allowed by combination of equation (1), (2) and (3).

$$[GltH_2]=\frac{[H^+]^2}{B}$$

$$[GltH^-]=\frac{K_1[H^+]}{B}$$

$$[Glt^{2-}]=\frac{K_1K_2}{B}$$

where B is given by following equation:

$$B=[H^+]^2+K_1[H^+]+K_1K_2$$

Effect of immersion time on adsorption of Glu.

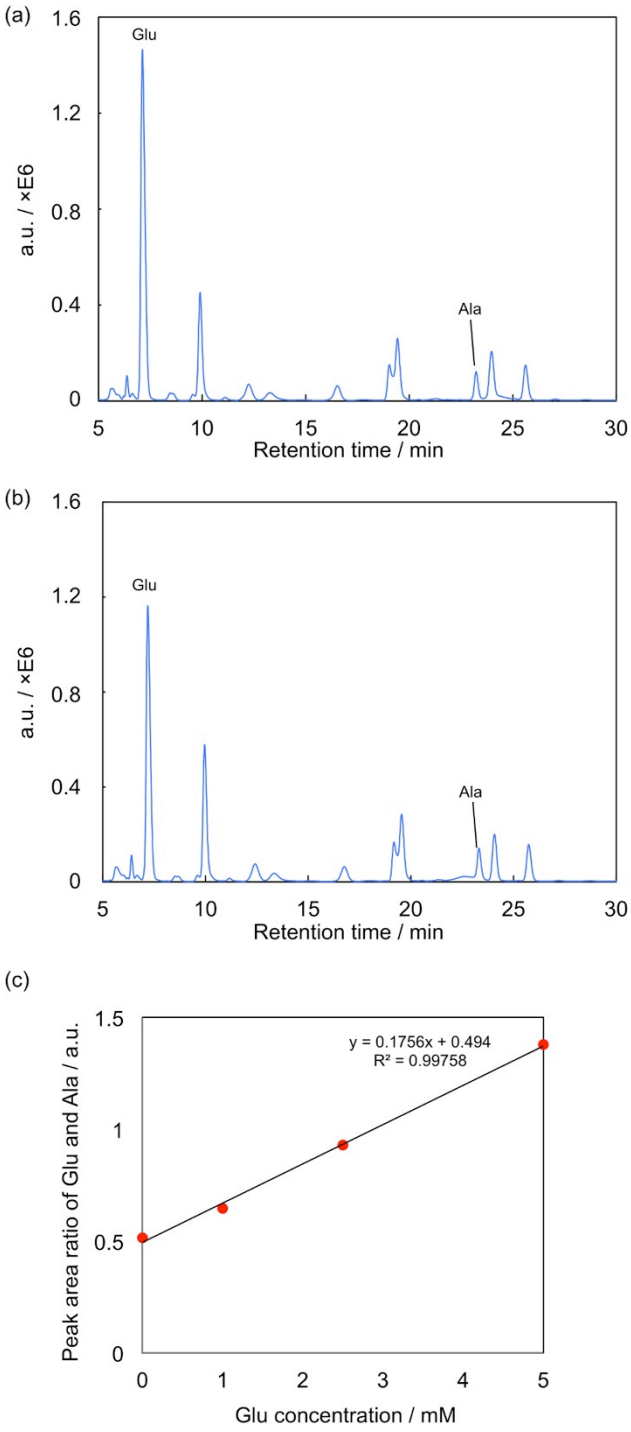

Fig. S3. (a) Chromatograms on initial concentration of Glu (50 mM). (b) Chromatogram data of Glu adsorption into $[Al(OH)(2,6\text{-ndc})]_n$ from 50 mM of Glu solution. (c) Calibration curve of Glu/Ala. Peaks of Glu and Alanine (Ala) were detected at around 7 min and 23 min, respectively. Peak area ratio of Glu to Ala obviously decreased because of adsorption of Glu after immersion of PCPs in 50 mM of Glu solution for various times up to 24 h. The calibration curve, which was determined by plotting peak of Glu as a function of concentration, assisted to calculate Glu concentration.

.

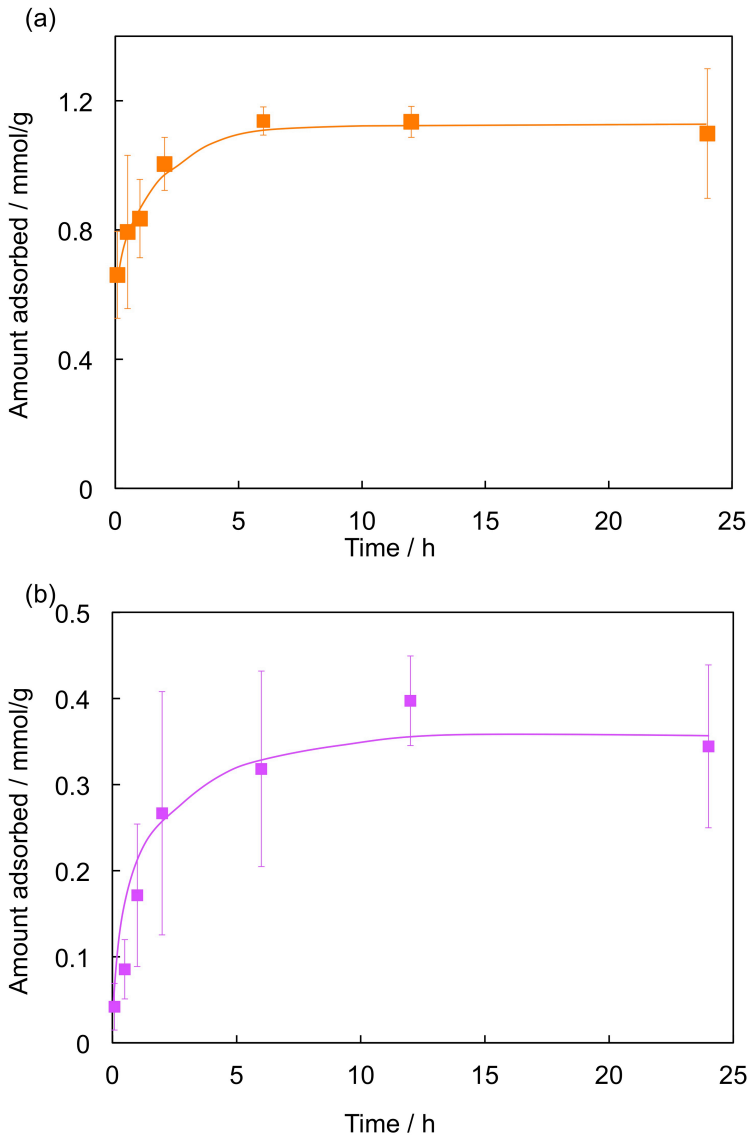

Fig. S4. Plot of adsorbed mount of Glu in (a) $[Al(OH)(1,4\text{-bdc})]_n$ and (b) $[Al(OH)(1,4\text{-ndc})]_n$ versus time. The adsorption experiment was carried out at 27 °C (pH = 3.3). The trend lines were drawn by hand to guide the eyes. Each dot represents a mean ± S.D. (n = 3). Adsorption amount on various times was determined by subtraction of equilibrium concentration from initial concentration of Glu. Glu adsorption amount increased to 1.12 and 0.34 mmol/g as increasing the immersion time and reached equilibrium at 12 h on both cases of $[Al(OH)(1,4\text{-bdc})]_n$ and $[Al(OH)(1,4\text{-ndc})]_n$, respectively. Note that no degradation was confirmed even after 24 h.

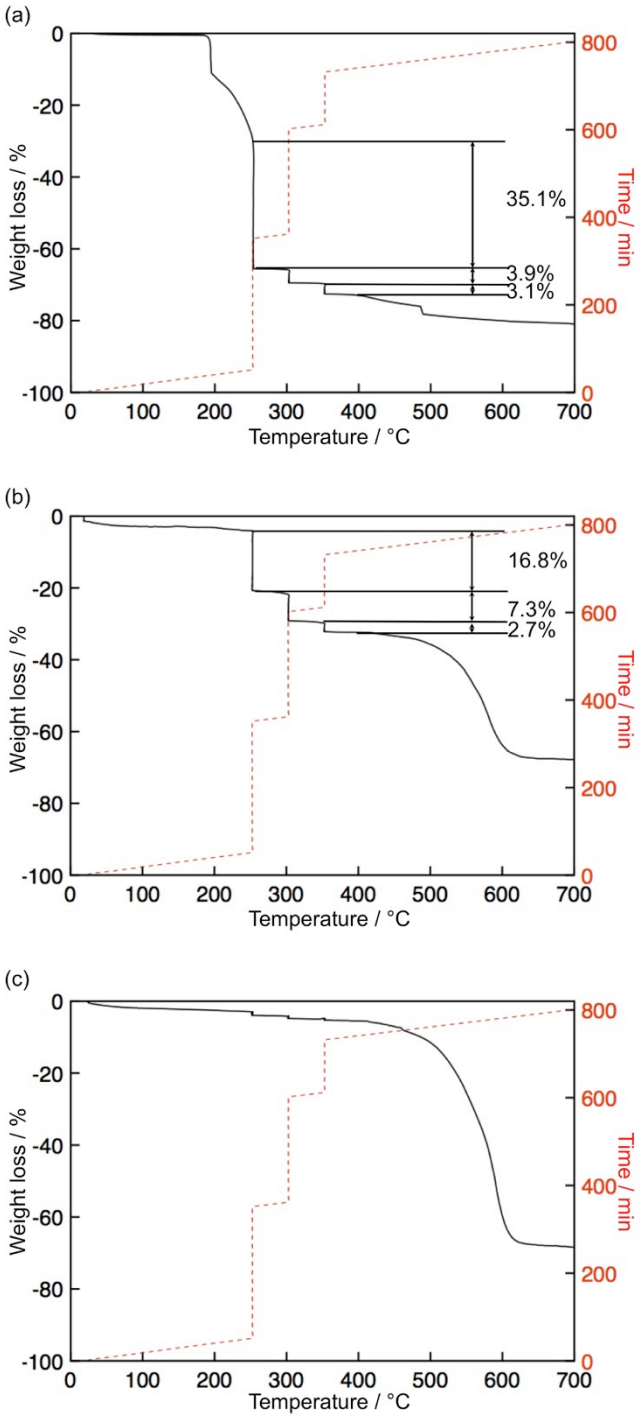

Fig. S5. Stepwise isothermal TGA curves of (a) Glu, (b) Glu@$[Al(OH)(2,6\text{-ndc})]_n$ (Glu was loaded at pH = 3.3) and (c) activated $[Al(OH)(2,6\text{-ndc})]_n$. The single step loading experiments were carried out. Dot line represents the change of time versus temperature.

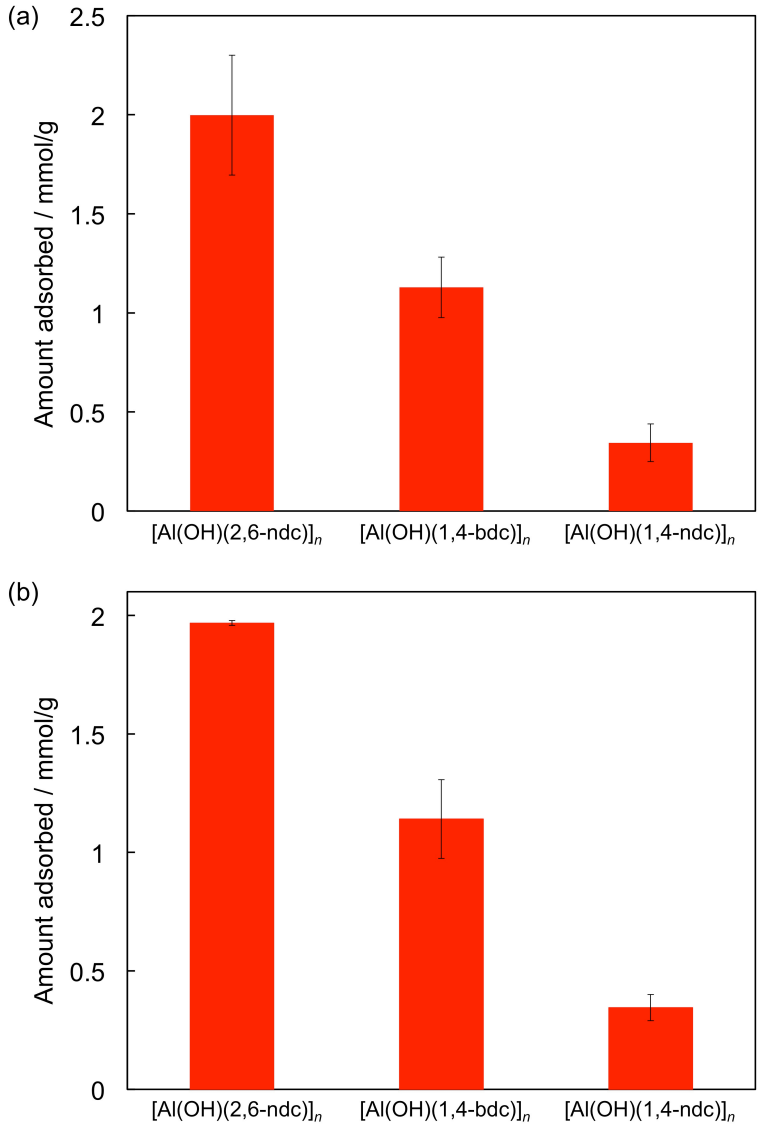

Fig. S6. (a) Amounts of Glu molecules loaded into the series of isoreticular $[Al(OH)(L)]_n$ frameworks. The two-step loading experiment was carried out for each framework at pH = 3.3 and the amounts were estimated by HPLC. (b) Amounts of Glu molecules loaded into the series of isoreticular $[Al(OH)(L)]_n$ frameworks. The two-step loading experiment was carried out for each framework at pH = 3.3 and the amounts were estimated by TGA. Each bar represents a mean ± S.D. (n = 3). The amount adsorbed was led by subtracting the concentration of Glu solution after adsorption from initial concentration. The adsorption amount of Glu into $[Al(OH)(L)]_n$ analyzed by HPLC corresponded to that determined by TGA.

Table S1. Comparison of HPLC results with TGA results on Glu adsorption into the PCP by single step loading.

	Glu adsorption amount (mmol/g)	
	HPLC results	TGA results
$[Al(OH)(2,6\text{-ndc})]_n$	1.99	1.96
$[Al(OH)(1,4\text{-bdc})]_n$	1.12	1.14
$[Al(OH)(1,4\text{-ndc})]_n$	0.34	0.34

The effect of pH on Glu adsorption in $[Al(OH)(L)]_n$.

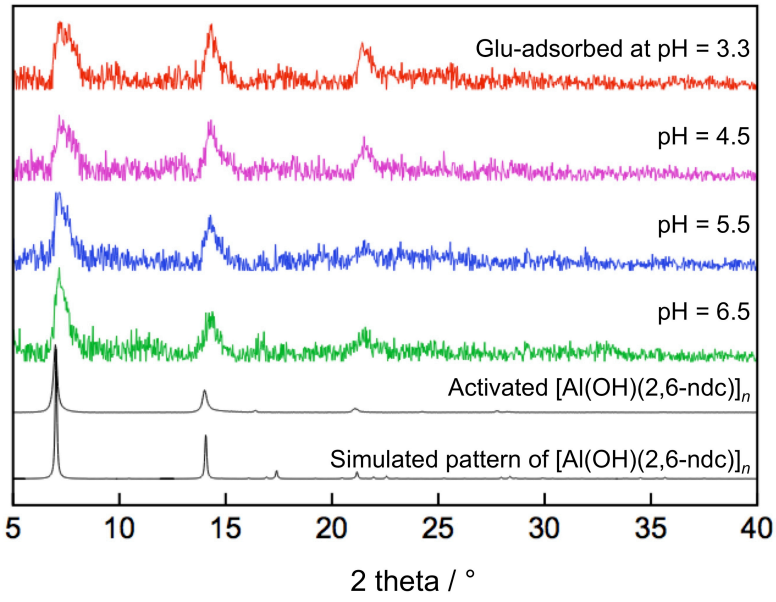

Fig. S7. PXRD patterns of $[Al(OH)(2,6\text{-ndc})]_n$ after the two-step Glu loading experiments under various pH conditions: pH = 3.3, pH = 4.5, pH = 5.5 and pH = 6.5. PXRD pattern of activated $[Al(OH)(2,6\text{-ndc})]_n$ and simulated pattern of $[Al(OH)(2,6\text{-ndc})]_n$.

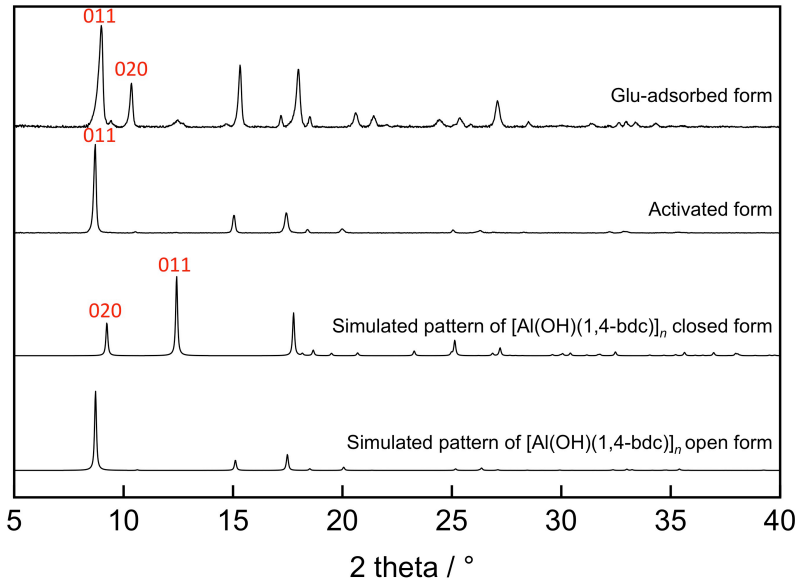

Fig. S8. PXRD pattern of $[Al(OH)(1,4\text{-bdc})]_n$ after the two-step Glu loading experiments at pH = 3.3 (as Glu-adsorbed form). PXRD pattern of activated $[Al(OH)(1,4\text{-bdc})]_n$ (as Activated form). Simulated patterns of closed and open forms of $[Al(OH)(1,4\text{-bdc})]_n$

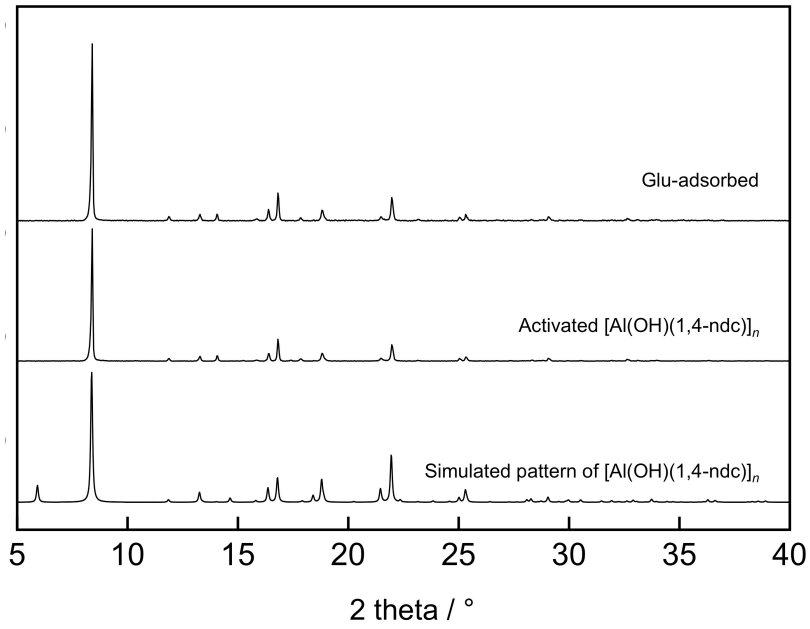

Fig. S9. PXRD pattern of $[Al(OH)(1,4\text{-ndc})]_n$ after the two-step Glu loading experiments at pH = 3.3 (as Glu-adsorbed form).. PXRD pattern of activated $[Al(OH)(1,4\text{-ndc})]_n$ and simulated pattern of $[Al(OH)(1,4\text{-ndc})]_n$.

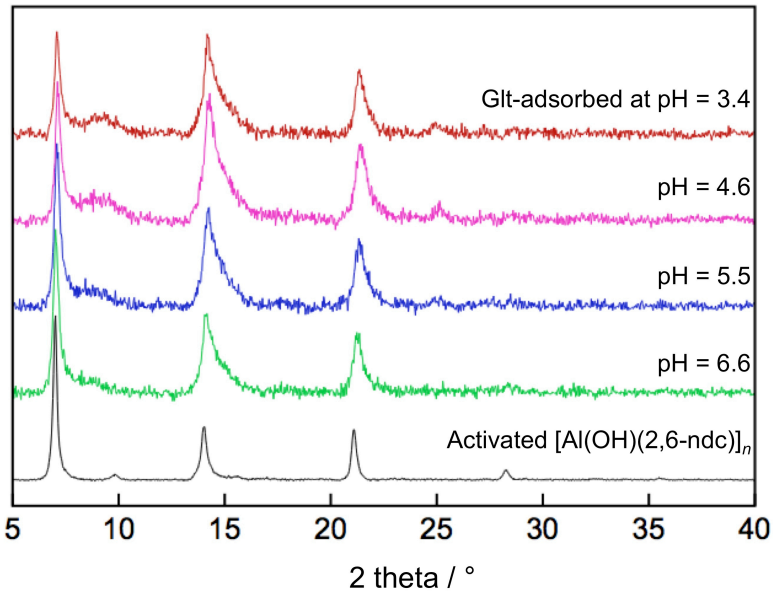

Fig. S10. PXRD patterns of $[Al(OH)(2,6\text{-ndc})]_n$ after the two-step Glt loading experiments under various pH conditions pH: pH = 3.4, pH = 4.6, pH = 5.5 and pH = 6.6. PXRD pattern of activated $[Al(OH)(2,6\text{-ndc})]_n$.

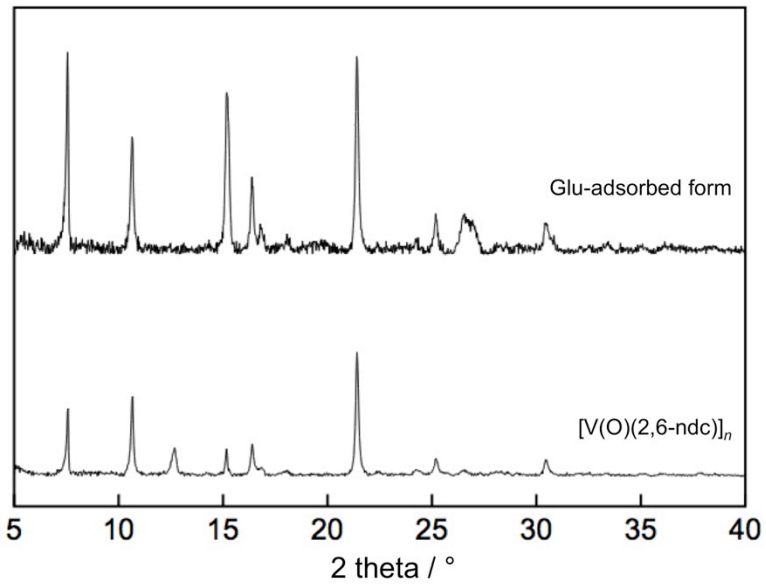

Fig. S11. PXRD pattern of $[V(O)(2,6\text{-ndc})]_n$ after the single step Glt loading experiments at pH = 3.3 (as Glu-adsorbed form). PXRD pattern of $[V(O)(2,6\text{-ndc})]_n$.

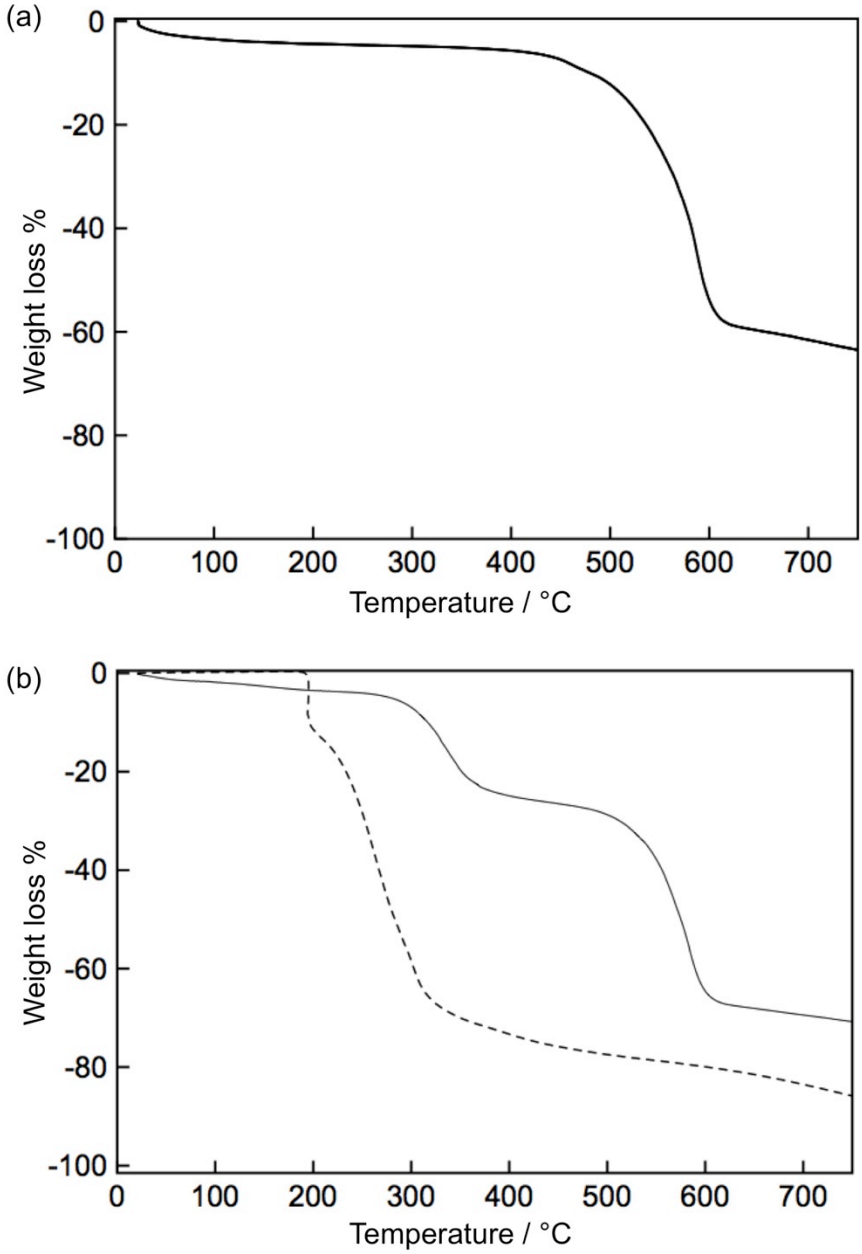

Fig. S12. TGA curves of (a) activated Al(OH)(2,6-ndc)]$_n$ and (b) Glu@[Al(OH)(2,6-ndc)]$_n$,. The two-step loading experiment was carried out for each framework at pH = 3.3. Dot line represents TGA curve of Glu.

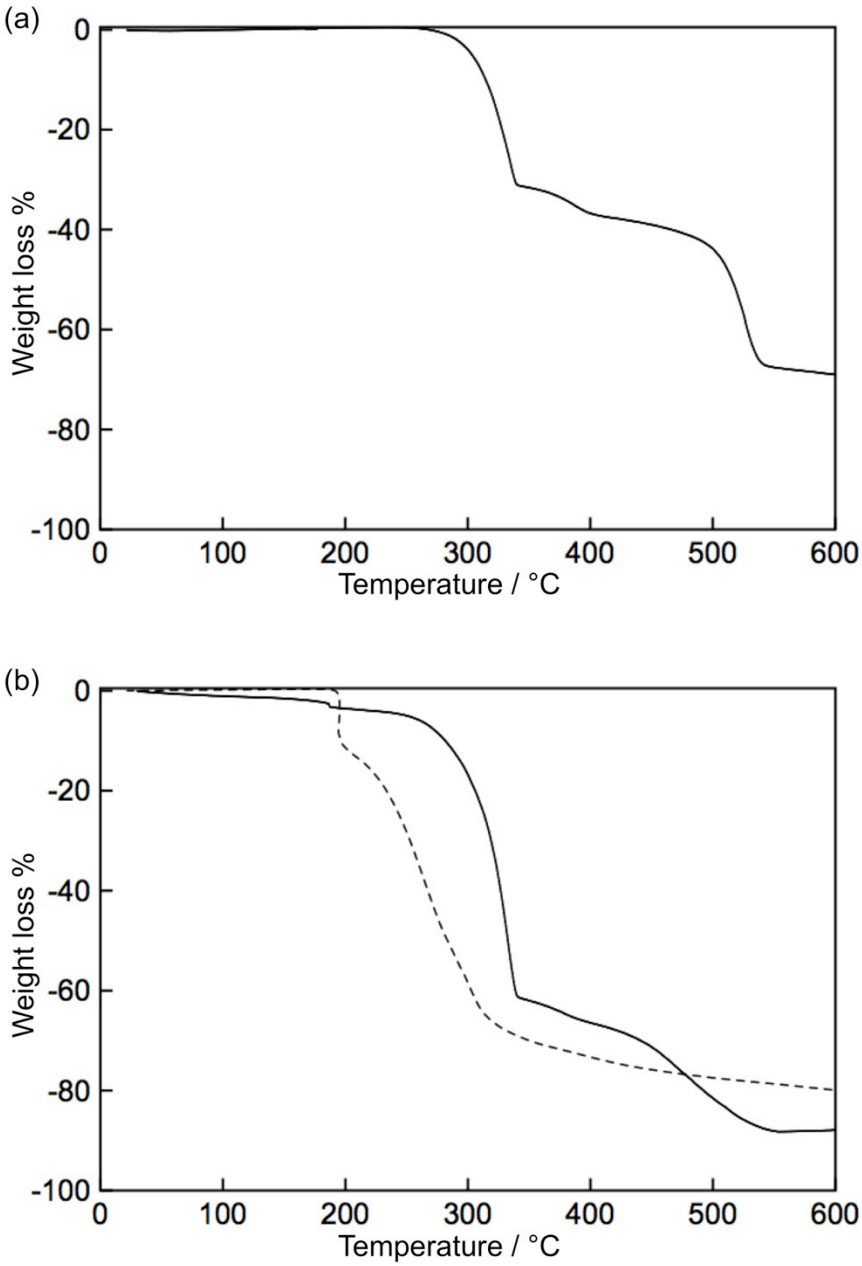

Fig. S13. TGA curves of (a) $[V(O)(2,6\text{-ndc})]_n$ and (b) Glu@$[V(O)(2,6\text{-ndc})]_n$. The two-step loading experiment was carried out for each framework at pH = 3.3. Dot line represents TGA curve of Glu. Because of overlapping the decomposition temperature of $[V(O)(2,6\text{-ndc})_n$ and Glu@$[V(O)(2,6\text{-ndc})_n$ at around 250 – 340 °C, the HPLC analysis was carried out to estimate Glu amount (See Figure S15 and Table S3).

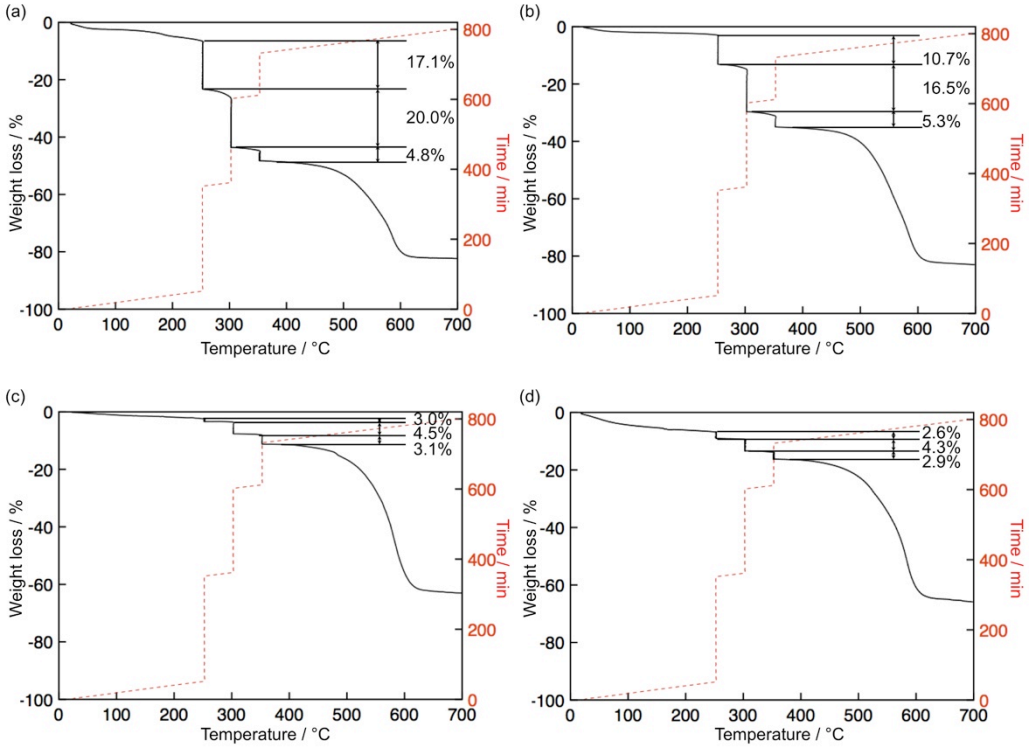

Fig. S14. Stepwise isothermal TGA curves of Glu@[Al(OH)(2,6-ndc)]$_n$. The two-step loading experiment was carried out for each framework at various pH: (a) pH = 3.3, (b) pH = 4.5, (c) pH = 5.5 and (d) pH = 6.5. Dot line represents the change of time versus temperature.

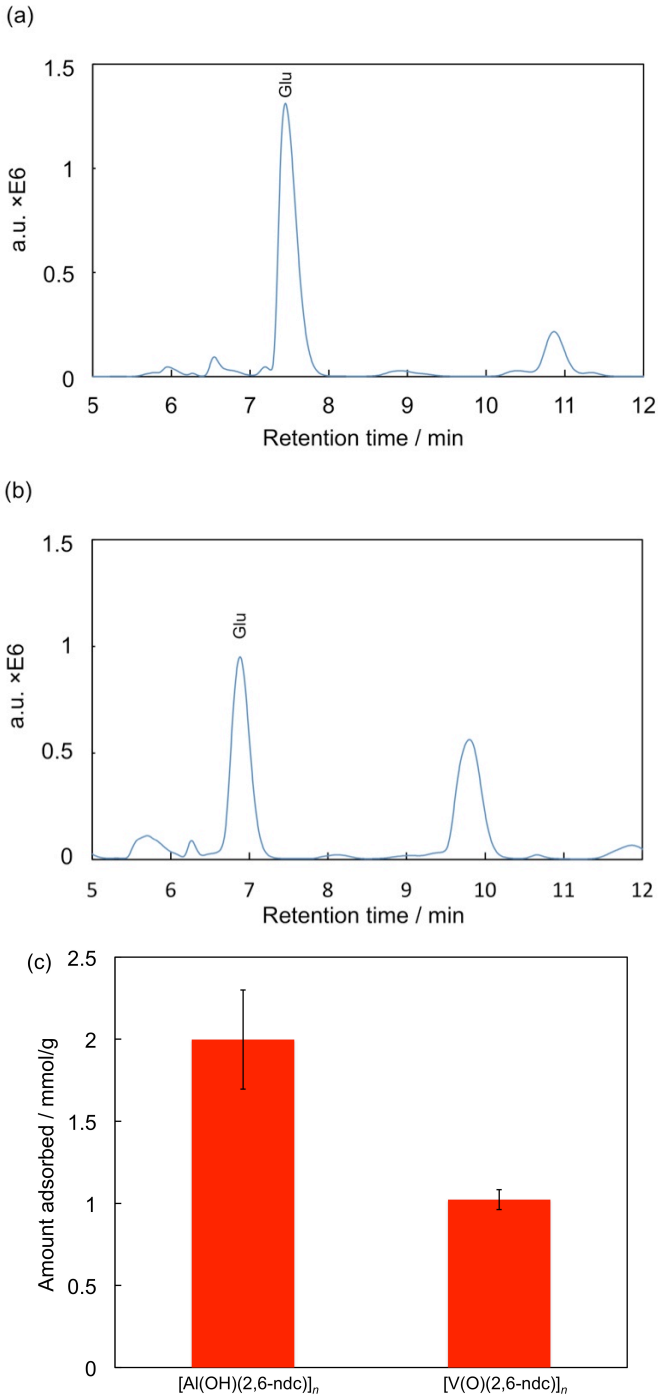

Fig. S15. (a) Chromatograms on initial concentration of Glu (50 mM). (b) Chromatogram data of Glu adsorption into $[V(O)(2,6\text{-ndc})]_n$ from 50 mM of Glu solution. (c) Amounts of Glu molecules loaded into $[Al(OH)(2,6\text{-ndc})]_n$ and $[V(O)(2,6\text{-ndc})]_n$. The two-step loading experiment was carried out for each framework at pH = 3.3 and the amounts were estimated by HPLC. Each bar represents a mean ± S.D. (n = 3). The investigation of adsorbed Glu into $[V(O)(2,6\text{-ndc})]_n$ was performed by following the same procedure of Fig. S6a.

Table S2 HPLC results on Glu adsorption into $[Al(OH)(2,6\text{-ndc})]_n$ and $[V(O)(2,6\text{-ndc})]_n$ by single step loading.

	$[Al(OH)(2,6\text{-ndc})]_n$	$[V(O)(2,6\text{-ndc})]_n$
Glu amount (mmol/g)	1.99	1.02

The effect of pore size of $[Al(OH)(L)]_n$ on Glu adsorption

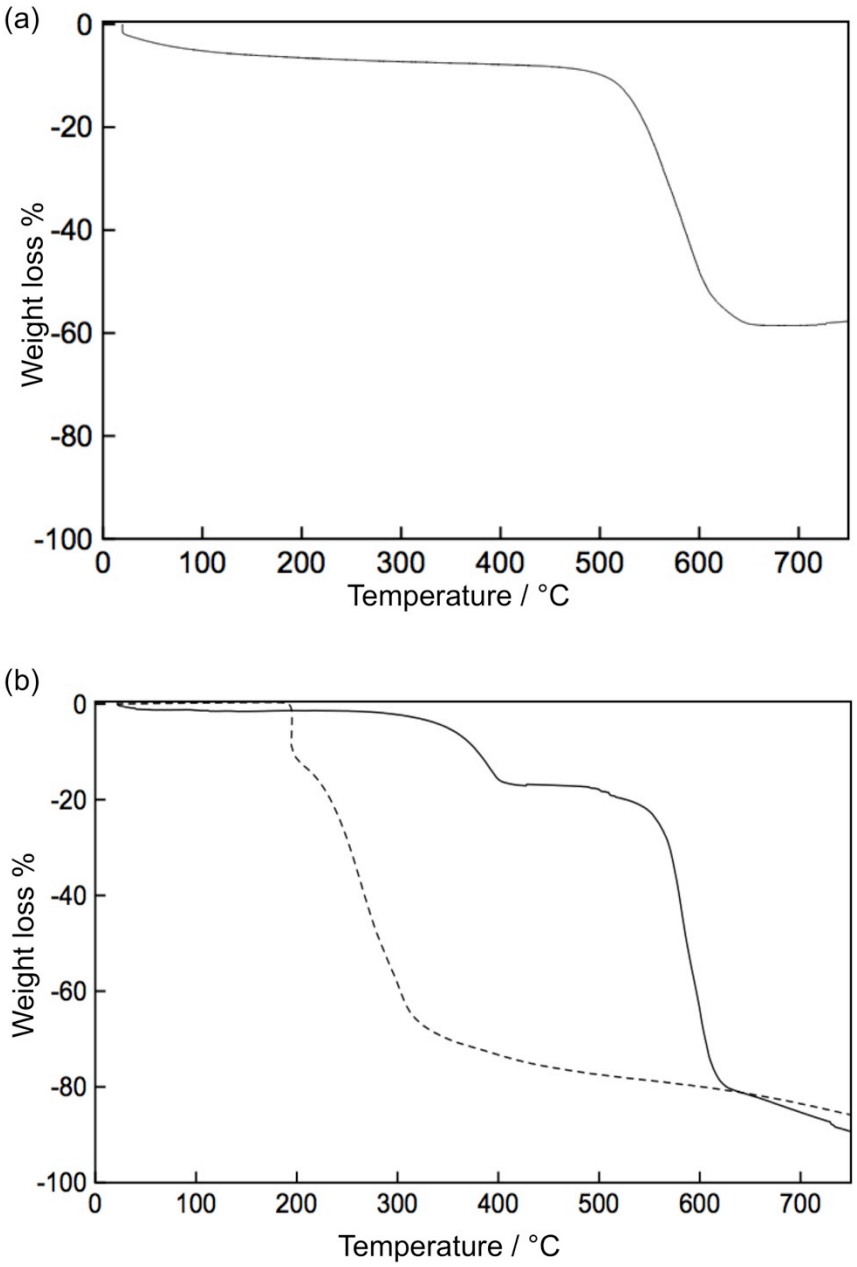

Fig. S16. TGA curves of (a) activated $[Al(OH)(1,4\text{-bdc})]_n$ and Glu@$[Al(OH)(1,4\text{-bdc})]_n$. The two-step loading experiment was carried out for each framework at pH = 3.3. Dot line represents TGA curve of Glu.

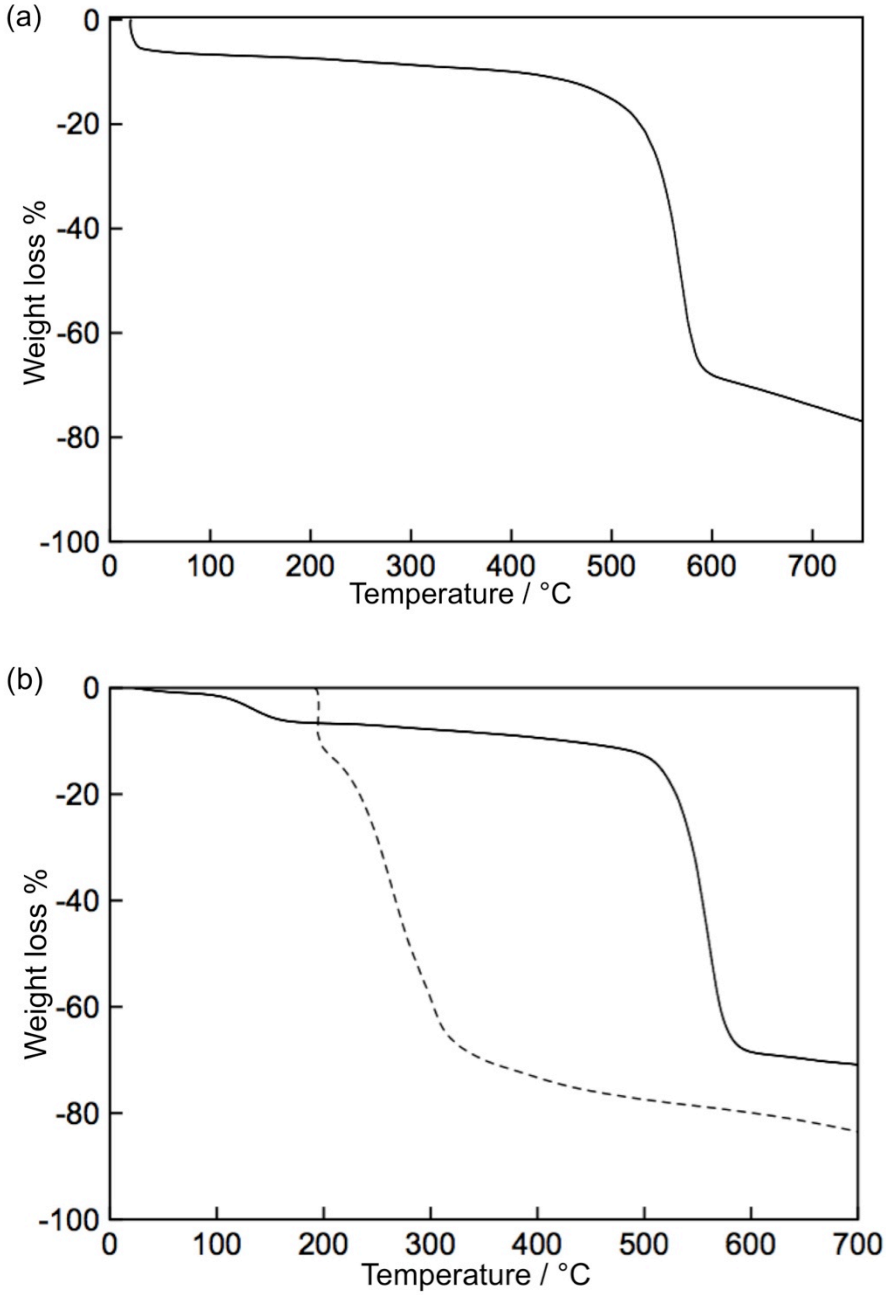

Fig. S17. TGA curves of (a) activated $[Al(OH)(1,4\text{-ndc})]_n$ and (b) Glu@$[Al(OH)(1,4\text{-ndc})]_n$. The two-step loading experiment was carried out for each framework at pH = 3.3. Dot line represents TGA curve of Glu.

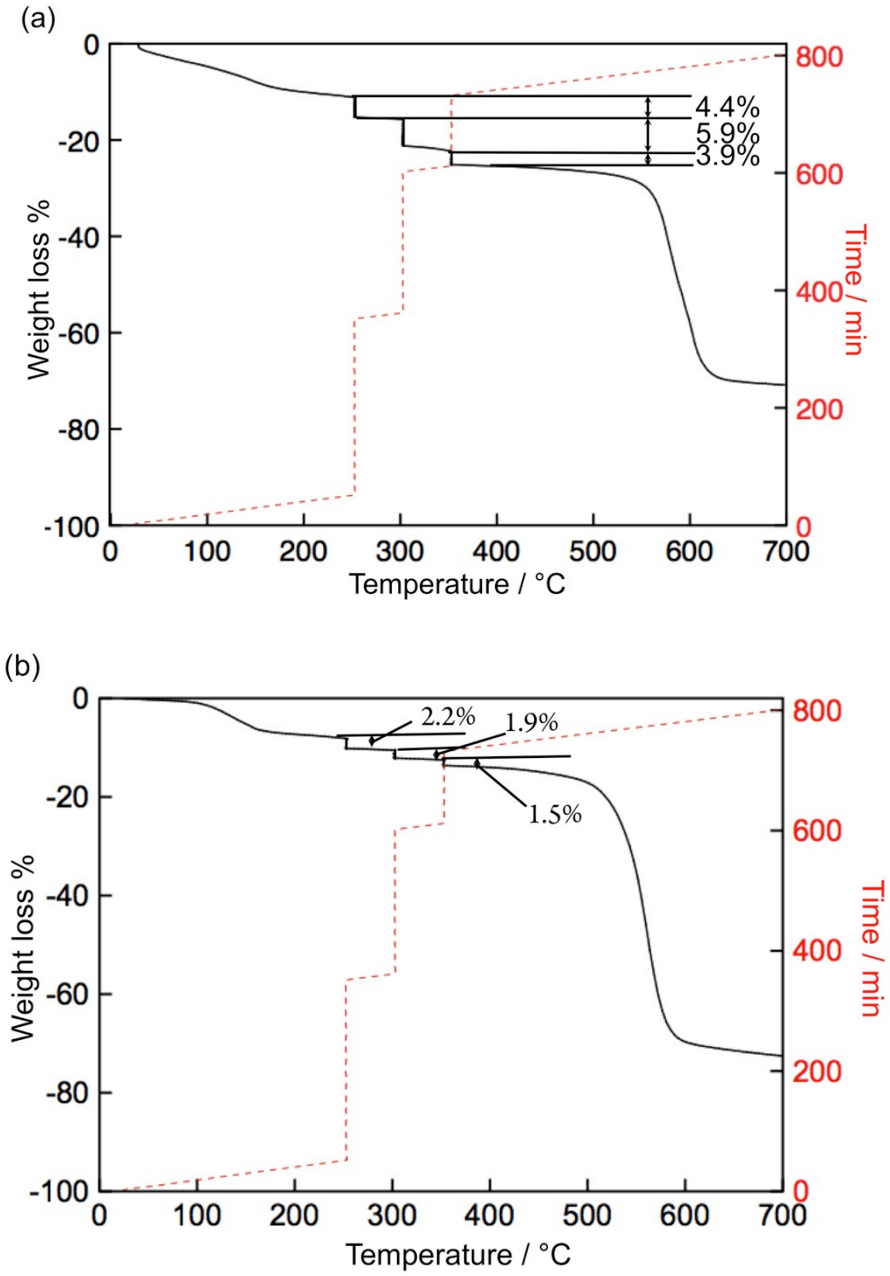

Fig. S18. Stepwise isothermal TGA curves of (a) Glu@[Al(OH)(1,4-bdc)]$_n$ and (b) Glu@[Al(OH)(1,4-ndc)]$_n$. The two-step loading experiment was carried out for each framework at pH = 3.3. Dot line represents the change of time versus temperature.

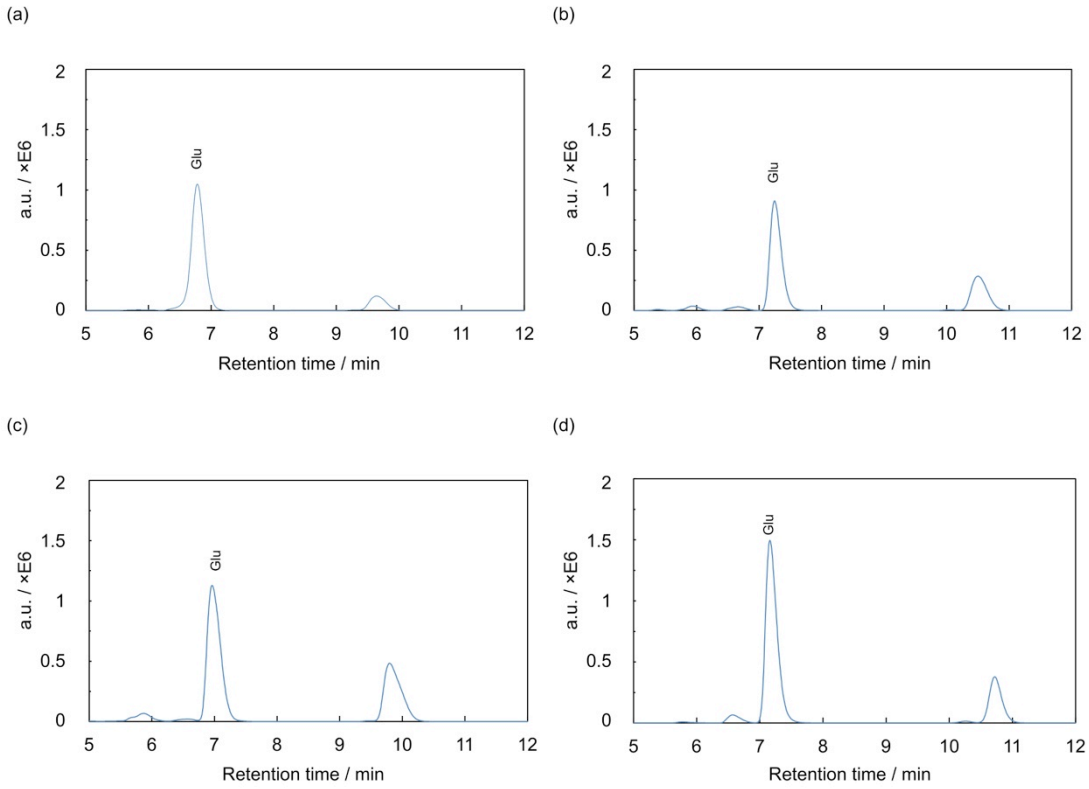

Fig. S19. Chromatograms of Glu adsorption into (a) $[Al(OH)(2,6\text{-ndc})]_n$, (b) $[Al(OH)(1,4\text{-bdc})]_n$ and (c) $[Al(OH)(1,4\text{-ndc})]_n$ from 5 mM of Glu solution. (d) Chromatogram data on initial concentration of Glu at 5 mM. No peak of organic ligand (at around 5.3 min) was detected by HPLC, hence no degradation of $[Al(OH)(L)]_n$ was occurred during the adsorption experiments. The peak area of Glu was decreased after immersion for 12 h. The Glu concentration was calculated by calibration curve, which was determined by relative peak area of Glu and Ala.

The release of Glu from $[Al(OH)(L)]_n$.

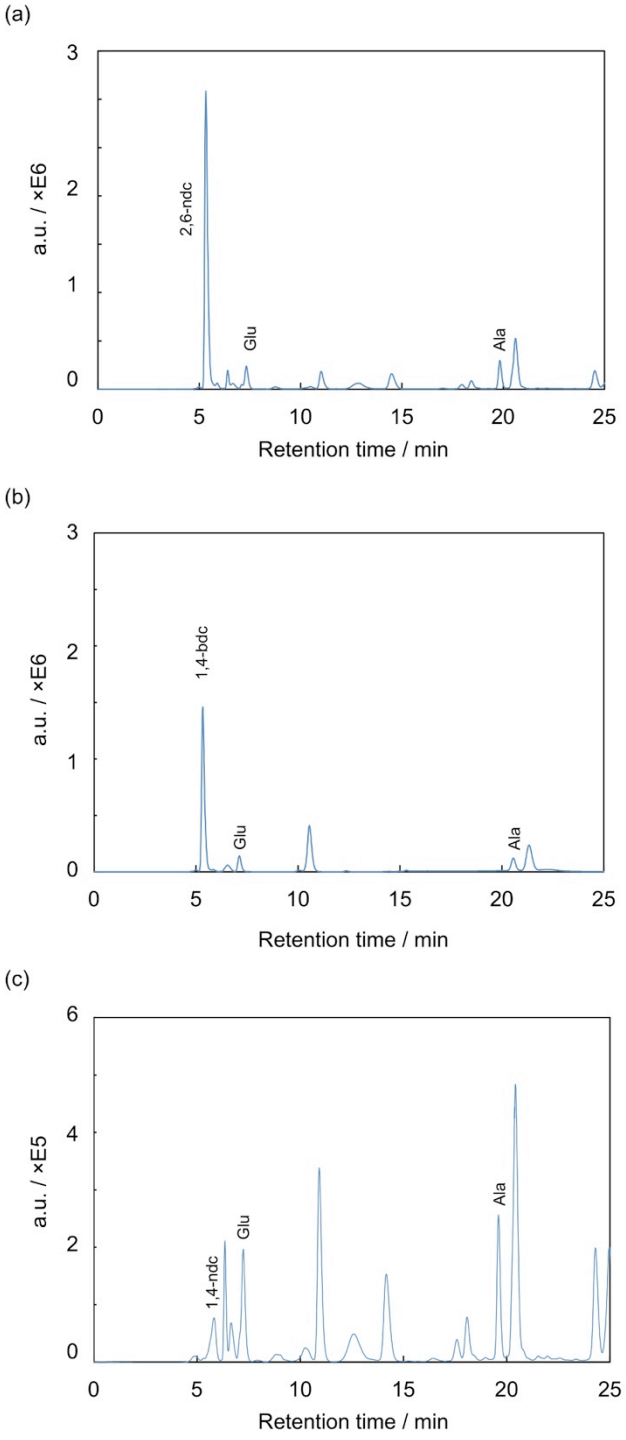

Fig. S20. Chromatograms of Glu, Ala, (a) 2,6-ndc, (b) 1,4-bdc and (c) 1,4-ndc in Tyrode's solution.

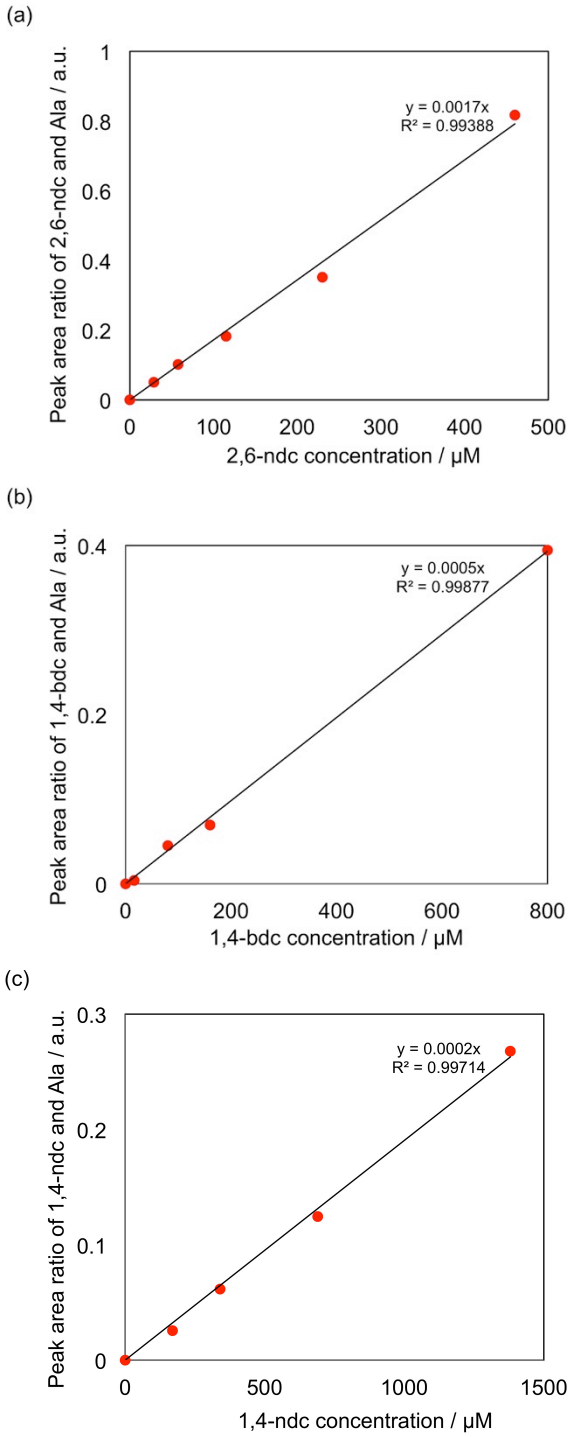

Fig. S21. Calibration curve of (a) 2,6-ndc/Ala, (b) 1,4-bdc/Ala and (c) 1,4-ndc/Ala in Tyrode's solution.

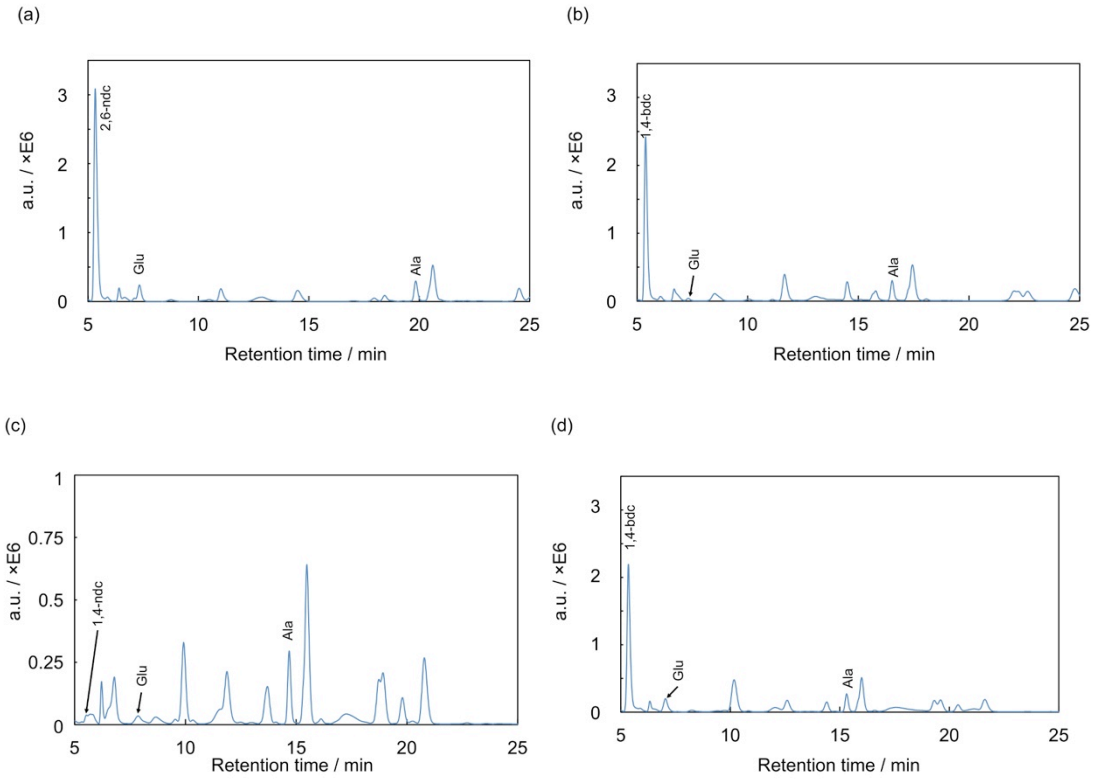

Fig. S22. Chromatograms of Glu release from (a) $[Al(OH)(2,6\text{-ndc})]_n$, (b) $[Al(OH)(1,4\text{-bdc})]_n$ and (c) $[Al(OH)(1,4\text{-ndc})]_n$ in Tyrode's solution at 37 °C after 12 h. Chromatograms of Glu release from (d) $[Al(OH)(1,4\text{-bdc})]_n$ in Tyrode's solution at 80 °C after 24 h. The Glu@$[Al(OH)(L)]_n$ composites were immersed in Tyrode's solution at 37 °C. The change of Glu release amount was chronologically monitored by reverse phase HPLC. In the case of $[Al(OH)(1,4\text{-bdc})]_n$, the peak of Glu was increased after heating up to 80 °C. The peaks of organic ligands were simultaneously detected with Glu peak at around 5.3 min, which implies that the degradation of $[Al(OH)(L)]_n$ occurs in physiological condition.

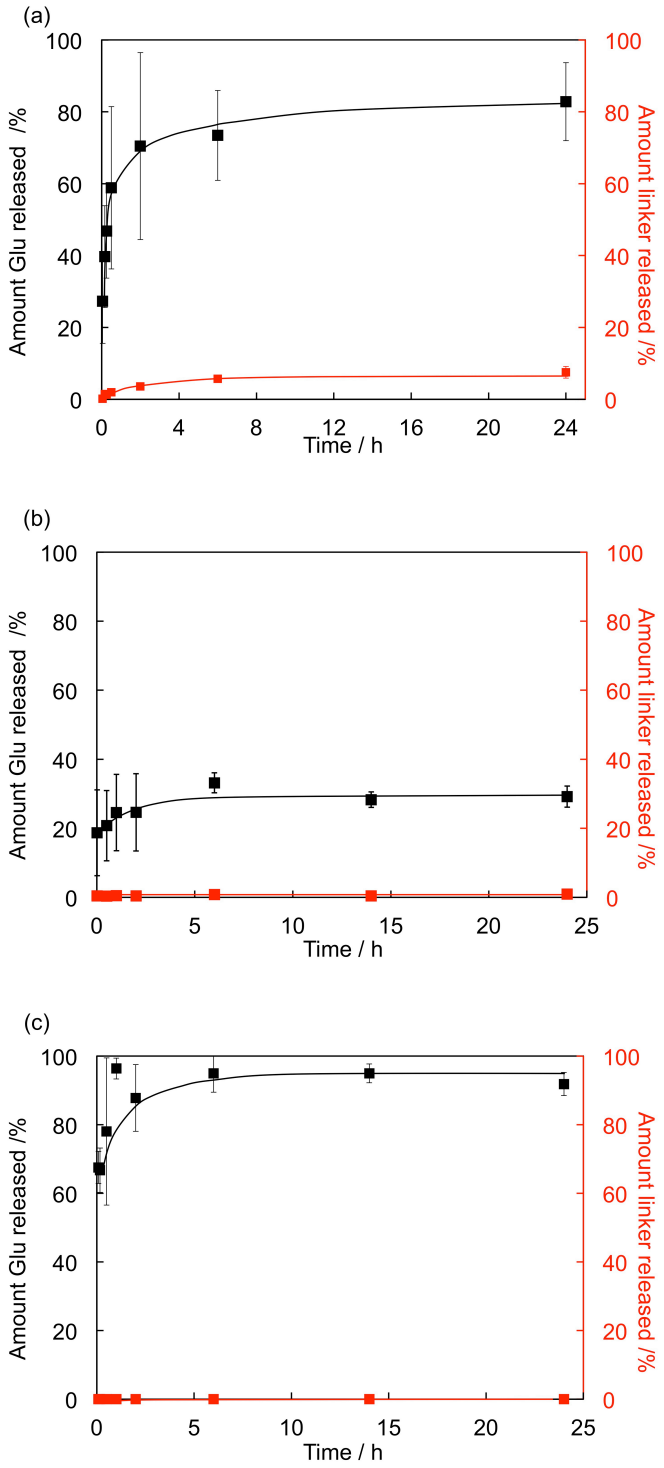

Fig. S23. Glu (black) and organic ligands (red) release from $[Al(OH)(L)]_n$ in Tyrode's solution at 37 °C. Each plot was analyzed by HPLC: (a) $[Al(OH)(2,6\text{-ndc})]_n$, (b) $[Al(OH)(1,4\text{-bdc})]_n$ and (c) $[Al(OH)(1,4\text{-ndc})]_n$. The trend lines were drawn by hand to guide the eyes. Each dot represents a mean ± S.D. (n = 3).

Table S3. Release amount of Glu and organic linkers from $[Al(OH)(L)]_n$ in Tyrode's solution at 37 °C after 24 h.

	Glu release amount % (mmol/g)	Linker release amount % (mmol/g)
$[Al(OH)(2,6\text{-ndc})]_n$	82.8 (2.4)	7.5 (0.29)
$[Al(OH)(1,4\text{-bdc})]_n$	29.1 (0.47)	0.93 (4.5×10^{-2})
$[Al(OH)(1,4\text{-ndc})]_n$	91.8 (0.30)	0 (0)

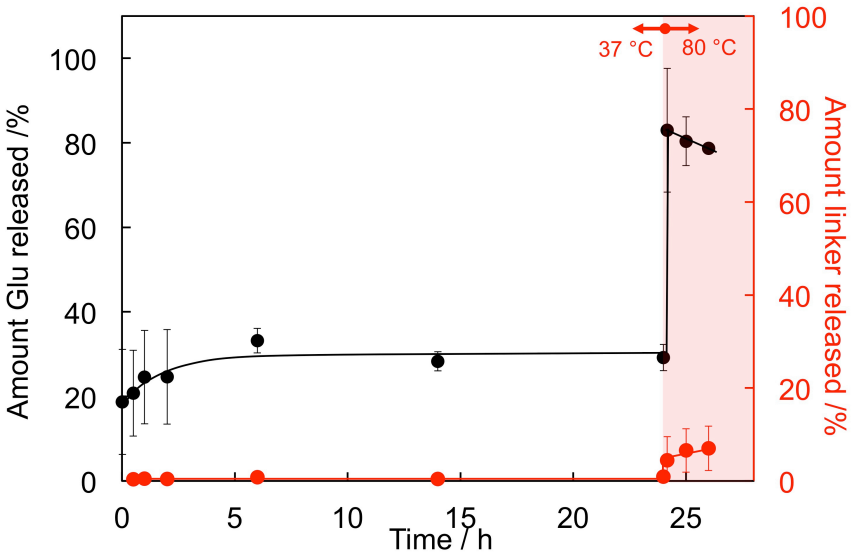

Fig. S24. Glu (black) and organic ligands (red) release from $[Al(OH)(1,4\text{-bdc})]_n$ in Tyrode's solution. The released amounts were estimated by HPLC. Significantly less amount of Glu (30%) was spontaneously released at 37 ºC. After 24 h, the temperature was increased up to 80 ºC and the burst release was observed. The trend lines were drawn by hand to guide the eyes. Each dot represents a mean ± S.D. (n = 3).

Table S4. Release amount of Glu and organic linkers from $[Al(OH)(1,4\text{-bdc})]_n$ in pure water at 37 °C after 24 h.

	Glu release amount % (mmol/g)	Linker release amount % (mmol/g)
Pure water	5.4 (0.08)	0.5 (0.02)

Table S5. Release amount of Glu and organic linkers from $[Al(OH)(1,4\text{-bdc})]_n$ in Tyrode's solution and pure water at 80 °C.

	Glu release amount % (mmol/g)	Linker release amount % (mmol/g)
Tyrode's solution	78.7 (1.28)	6.5 (0.33)
Pure water	7.2 (0.11)	0.5 (0.02)

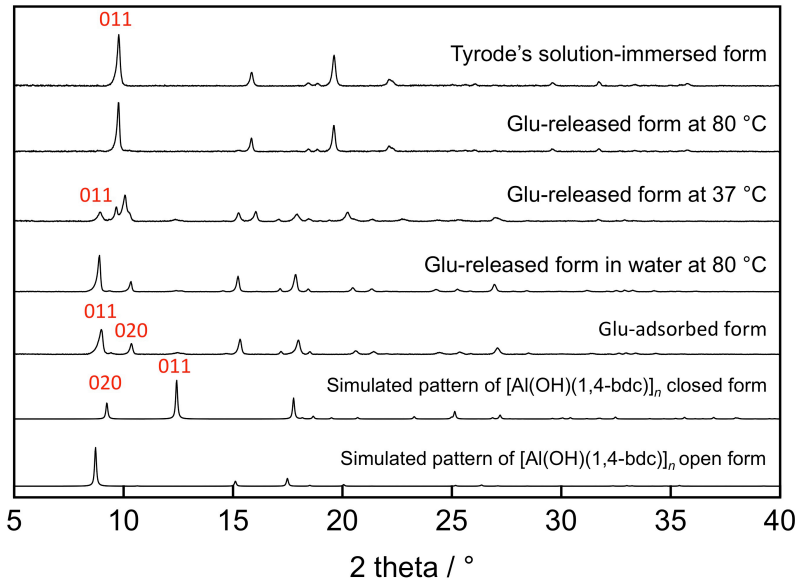

Fig. S25. PXRD patterns of $[Al(OH)(1,4\text{-bdc})]_n$ after releasing Glu in Tyrode's solution at 80 °C and 37 °C. PXRD patterns of $[Al(OH)(1,4\text{-bdc})]_n$ after immersion in Glu solution at pH = 3.3. Simulated pattern of closed form of $[Al(OH)(1,4\text{-bdc})]_n$ and of open form of $[Al(OH)(1,4\text{-bdc})]_n$.

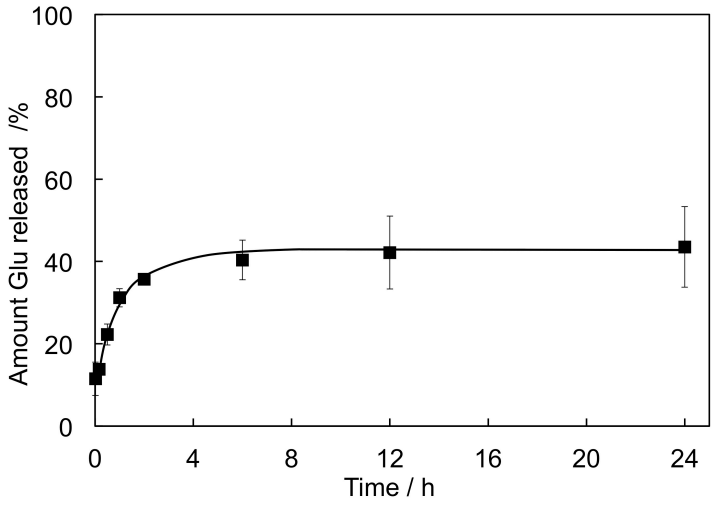

Fig. S26. Plots of released amount of Glu from $[Al(OH)(2,6\text{-ndc})]_n$ versus time in pure water at 37 °C. The released amounts were estimated by HPLC. The trend line was drawn by hand to guide the eyes. Each dot represents a mean ± S.D. (n = 3).

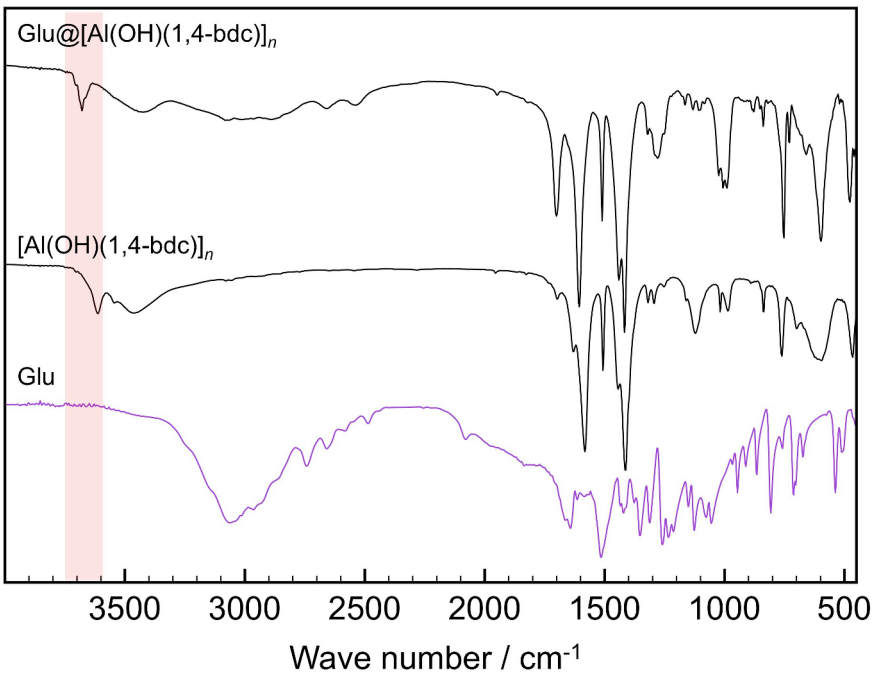

Fig. S27. IR spectra of Glu@[Al(OH)(1,4-bdc)]$_n$, [Al(OH)(1,4-bdc)]$_n$ and Glu.